Published in final edited form as:
Circulation. 2018 January 30; 137(5): 488–503. doi:10.1161/CIRCULATIONAHA.117.028533.

Chronic rejection of cardiac allografts is associated with increased lymphatic flow and cellular trafficking

Lindsey A. Edwards, Ph.D.[1], **Anna K Nowocin, Ph.D.**[1], **Nazila V. Jafari, Ph.D.**[1], **Lucy L. Meader, MRes**[1], **Kathryn Brown, Ph.D.**[1], **Aurélien Sarde, M.Sc.**[1], **Carolyn Lam, BSc**[1], **Alex Murray, BSc**[1], and **Wilson Wong, MRCP, DPhil**[1,2]

[1]MRC Centre for Transplantation, King's College London, Guy's Hospital, London, United Kingdom

[2]King's College London, School of Medicine at Guy's, King's and St. Thomas' Hospitals, London, United Kingdom

Abstract

Background—Cardiac transplantation is an excellent treatment for end-stage heart disease. However, rejection of the donor graft, particularly by chronic rejection leading to cardiac allograft vasculopathy, remains a major cause of graft loss. The lymphatic system plays a crucial role in the alloimmune response, facilitating trafficking of antigen presenting cells (APCs) to draining lymph nodes (dLN). The encounter of APCs with T lymphocytes in secondary lymphoid organs is essential for the initiation of alloimmunity. Donor lymphatic vessels are not anastomosed to that of the recipient during transplantation. The pathophysiology of lymphatic disruption is unknown and whether this disruption enhances or hinders the alloimmune responses is unclear. Although histological analysis of lymphatic vessels in donor grafts can yield information on the structure of the lymphatics, the function, however, following cardiac transplantation is poorly understood.

Methods—Using Single photon emission computed tomography/CT (SPECT/CT) lymphoscintigraphy, we quantified the lymphatic flow index (LFI) following heterotrophic cardiac transplantation in a murine model of chronic rejection.

Results—Ten weeks following transplantation of a minor antigen (HY) gender-mismatched heart graft, the LFI was significantly increased compared with gender-matched controls. Furthermore, the enhanced LFI correlated with an increase in donor cells in the mediastinal dLN; increased lymphatic vessel area; and graft infiltration of $CD4^+$, $CD8^+$ T-cells and $CD68^+$ macrophages.

Conclusions—Chronic rejection results in increased lymphatic flow from the donor graft to dLNs, which may be a factor in promoting cellular trafficking, alloimmunity, and cardiac allograft vasculopathy.

Correspondence: Dr. Wilson Wong DPhil. King's College London, School of Medicine at Guy's, King's and St. Thomas' Hospitals, MRC Centre for Transplantation, 5th Floor Tower Wing, Guy's Hospital, London SE1 9RT. Fax: +44(0)2071885660. Tel: +44(0)2071881522. wilson.wong@kcl.ac.uk; Dr. Lindsey Ann Edwards, E-mail: lindsey.edwards@kcl.ac.uk, Twitter handle: @DrLAEdwards.

Disclosures
The authors have no conflicts of interest to disclose

Europe PMC Funders Author Manuscripts

Keywords

Transplantation; rejection; immune system; inflammation

Europe PMC Funders Author Manuscripts

Introduction

Heart transplantation is currently the best treatment for patients with end-stage heart failure. With the development of more potent immunosuppression, the one-year survival rate has risen to 85% in the UK1. However, immunosuppressive drugs have several metabolic, infectious, renal and neoplastic side effects2 and have not prevented the development of cardiac allograft vasculopathy (CAV); the main limitation of long-term survival of heart transplant recipients3–5. Histologically, CAV presents as a complex interplay between proliferative myoblasts, macrophages and T-lymphocytes leading to the formation of a neo-intima5. There is a need to understand the factors that are responsible for CAV in order to develop targeted treatment to prevent it.

Following heart transplantation, the cytokine milieu that results due to ischemia/reperfusion injury activates donor passenger leukocytes (DPL) to migrate out of the graft6. DPL can traffic in the blood circulation to the spleen *via* reverse transmigration where they can elicit an immune response7. Alternatively, they can traffic to draining lymph nodes (dLN) *via* lymphatic vessels. During transplantation, donor lymphatic vessels are not reconnected to that of the recipient, this period coincides with the priming of the alloimmune response8. It is hypothesised that the accelerated coronary atherosclerosis seen in heart transplant recipients is a result of this interrupted lymphatic drainage after surgery9. Our laboratory has demonstrated that DPL exit the donor graft *via* the severed ends of donor lymphatics vessels are taken up by recipient lymphatic capillaries and traffic to recipient dLN where they elicit a donor-specific T-cell-driven immune response8.

In our model of mouse heterotopic cardiac transplantation, reconnection of donor lymphatic vessels to those of the recipient occurred by four weeks8. In the context of inflammation, remodelling of lymphatics within the donor organ post-transplantation occurs by lymphangiogenesis and can be divided into (i) re-connection of donor lymphatics to that of the recipient, and (ii) *de novo* neogenesis10–12, due to infiltration of macrophages expressing LYVE-1, Prox-1, VEGFR-3, and VEGF-C12. Both mechanisms are likely to influence the lymphatic flow rate from the donor graft, which may influence the subsequent immune response. Studies of lymphangiogenesis have mainly focused on renal and corneal, rather than cardiac allograft models10, 11 or have not investigated lymphatic flow4, 13. Therefore, translation of the processes of lymphangiogenesis into a model of heterotrophic cardiac transplantation, in addition to the investigation of lymphatic flow, in this study is novel.

Although the density and size of lymphatic vessels in transplanted hearts have been shown to increase in preclinical models4, 13; its implication is not clear for clinical cardiac transplant samples, where increased lymphatic density has been linked to both rejection14, 15 and tolerance16. Crucially, whether lymphangiogenesis and increased lymphatic vessel density observed following cardiac transplantation does lead to increased lymphatic flow and

cellular trafficking is unknown, due to the lack of objective quantitative measurement of lymph flow after transplantation. While increased lymphatic vessel density could enhance DPL trafficking, antigen presentation, and alloimmunity; decreased lymphatic vessel density could lead to oedema, which accompanies acute organ rejection in many cases17. Whether changes in lymphatic density detected on histological studies are cause or effect of the immune process is unknown. Furthermore, the effects of transplant rejection itself on the structure, and more importantly, the function of lymphatic vessels remains unclear. Therefore, whether lymphangiogenesis is beneficial or detrimental to graft survival is not clear.

Here, we used SPECT/CT lymphoscintigraphy to provide objective quantification of lymphatic flow in a pre-clinical model of chronic heart transplant rejection and correlated it with graft damage and inflammatory infiltrates to investigate the link between functional lymphatic flow and the alloimmune process.

Methods

Animals

C57BL/6 (H-2^b) mice were purchased from Harlan UK Ltd. (Oxon, UK). C57BL/6 (H-2^b) mice expressing the enhanced yellow fluorescent protein targeted to the ROSA-26 locus (ROSA-EYFP)18, 19 in which EYFP is expressed ubiquitously, were bred in house. Animals were kept in specific pathogen-free animal facilities and used in accordance with the Animals (Scientific Procedures) Act 1986.

Cardiac transplantation

Heterotopic cardiac allografts into the abdomen were performed as previously described20, 21 and grafts were monitored by palpation22 (see supplementary methods).

Single Photon Emission Computed Tomography/CT (SPECT/CT) lymphoscintigraphy

At one, five or ten weeks after transplantation, under general anaesthesia, the donor hearts were exposed. Nanocoll (GE Healthcare, Buckinghamshire, UK), consisting of 30MBq of Technetium-99m (Tc-99m) labelled human albumin nanoparticle in 0.1 mL saline, was injected directly into the left ventricular wall at the apex. Injection of nanocoll is a validated approach to detect lymphatic flow in humans. The incision was then closed and the animals positioned in a nanoSPECT/CT preclinical imager (Bioscan Inc. Washington, DC, USA) imaged as described previously8. SPECT/CT images are taken after injection of nanocoll into the apex of transplanted hearts. After the final scan, the mice were sacrificed and the donor heart graft and the recipient's dLN were harvested. Using the Invivoscope software (Bioscan, Inc.) a sphere is drawn around each "region of interest" for quantification of the level of radioactivity within the sphere (Figure 1j; blue & red sphere). The concentration of radiation determined (Invivoscope software) to be present (MBq) at both scan times is decay corrected to the initial time of the injection of the Nanocoll. The decay corrected values are used to quantify the lymphatic flow index (Figure 1k). Heterotopic transplantation of donor hearts in this model results in donor lymph draining into the mediastinal (m)dLN of the recipients. Scanning of heart recipients at multiple time points after injection of Nanocoll

allows quantification of the rate of accumulation of radioactivity in the mdLN as a percentage of the injected dose into the myocardium, providing an objective measurement of lymphatic function, the lymphatic flow index (LFI) (Figure 1j-l). Although this does not give an absolute measurement of lymphatic flow, it provides an objective quantitative assessment of the lymphatic function of the transplanted organ.

Evan's Blue dye injection

Ten μL of 0.5%w/v Evans Blue (Sigma-Aldridge, Dorset UK) dye was injected into the left ventricular wall of the donor hearts at the apex. Twenty minutes later, the recipient mouse was dissected to directly visualise the pattern of lymph drainage so that the dLN could be identified.

Immunohistochemistry

Donor grafts were harvested and processed for immunohistochemistry; sections were stained with antibodies against CD4 (BD Pharmingen, Oxford, UK), CD8 (BD Pharmingen), CD68 (Serotec, Oxford, UK), or LYVE1 (Abcam plc, Cambridge, UK), as previously described23 (see supplementary methods). To determine the cross-sectional area of the lymphatic vessels. Images of MPF were analysed with Image J software. To determine if vessels were of donor or recipient in origin, staining of lymphatic vessels was performed using a modified protocol. The recipient EYFP cell signal was amplified with FITC conjugated goat anti-YFP (Abcam plc) as described in the supplementary methods.

Histology

Donor heart graft tissue was harvested and graft vasculopathy was confirmed by Elastic Van Gieson staining (Sigma-Aldridge), which was carried out per manufacturer's instructions as described previously5 (see supplementary methods).

Quantitative PCR

Genomic DNA from dLNs was isolated using a DNeasy Blood & Tissue extraction kit per the manufacture’s instructions (Qiagen, Manchester, UK). DNA concentration was quantified with a Nanodrop ND-1000 spectra-photometer. The Y-chromosome specific gene, Zfy1, was amplified using quantitative Real-time PCR. The presence of male donor-derived cells in the female recipient dLN was calculated against a standard curve of a known percentage of male DNAs as previously reported 24, 25 (See supplementary methods).

Statistics

Normality of distributions was calculated using the D'Agostino & Pearson and the Shapiro-Wilk normality tests to determine further statistical analysis. For figure one, the Mann-Whitney U test was used to test for significance between the LFI and loss of radiation from the graft between HY mismatched and gender-matched transplant recipients. For figures, two to four, the Student T-test was used to test for statistical differences between lymphatic vessel size and area and infiltrating inflammatory cell scores from different experimental groups. The statistical differences between time points for these data sets were analysed by a two-way Anova. Allograft immunohistochemical and genomic data was correlated to LFI

using regression analyses (linear, R^2) and the Spearman rank correlation coefficient (r_s), using GraphPad Prism 7 (GraphPad Software, San Diego, CA, USA). Groups ranged from n=4 to 7.

Results

Increased Lymphatic flow index in minor antigen mismatched heart grafts undergoing chronic rejection

Although structural changes of lymphatic vessels in donor grafts have been documented, objective measurement of the lymphatic function is lacking. We, therefore, used SPECT/CT lymphoscintigraphy developed in our laboratory8 and extended it to give quantitative data on lymphatic flow after transplantation. SPECT/CT lymphoscintigraphy was performed on female EYFP C57BL/6 recipient *mice* that have received either wild type male or gender-matched C57BL/6 donor hearts (Figure 1). Gender-mismatched male grafts express the male antigen HY, a minor histocompatibility antigen recognised by the female recipient. This antigen evokes a chronic rejection response26, resulting in CAV.

Recipients underwent injection of Nanocoll directly into the donor myocardium at the apex and SPECT/CT lymphoscintigraphy. At week one, re-connection of donor lymphatic vessels to that of the recipient will not have occurred. Scanning was also conducted at week five as we have previously shown reconnection of the donor lymphatic vessels occurred by four weeks8. Week ten was also chosen to study the effect of *de novo* neogenesis, within the donor graft, on lymphatic flow. Significant CAV would have developed by this time as well.

In this model, lymph flow from the donor organ drains into the mediastinal (m)dLN; which was observed at four hours, at week one, in the gender-matched grafts (Figure 1a) and HY-mismatch grafts (Figure 1b); in the HY-mismatch grafts at week five (Figure 1d, supplementary video 1) and ten weeks (Figure 1f). However, in the gender-matched grafts, no radioactivity was observed in the mdLN at week five (Figure 1c, supplementary video 2) or at ten weeks (Figure 1e).

To provide direct visual evidence of increased lymph drainage ten weeks after transplantation in HY-mismatched donor grafts compared with gender-matched grafts, Evan's blue, a dye used to track lymph flow was injected into the donor hearts at the apex instead of Nanocoll. Figure 1g-i shows that indeed the blue dye can be seen in mdLN above the native heart (white arrow) of recipients of HY-mismatched grafts (Figure 1g-h & Supplementary Figure 1, yellow arrows), but not in that of recipients of gender-matched grafts (Figure 1i).

Scanning of heart recipients at multiple time points after Nanocoll injection allows calculation of the rate of radioactivity accumulation into the mdLN (Figure 1j-k) and therefore the LFI (Figure 1l); in addition to quantifying the loss of radiation from the injected graft (Figure 1m). Figure 1l shows that the LFI is higher at one week following transplantation in both graph types, presumably due to enhanced lymphatic leakage *via* the severed donor lymphatics. The LFI was higher in the gender-matched grafts compared with the HY-mismatched grafts at 35.093 *vs.* 10.361 $x10^{-3}$ % $hour^{-1}$ respectively (p=0.0080;

Figure 1l). The situation is reversed at weeks five and ten (Figure 1l); where lymph flow from gender-matched grafts had virtually ceased. The LFI at week five was below the limit of detection 0 *vs.* 22.329 x10^{-3} % $hour^{-1}$, for the gender-matched *vs.* the HY-mismatched grafts respectively (p=0.0286), and at week ten, 0 *vs.* 0.88867 x10^{-3} % $hour^{-1}$, respectively (p=0.0156).

To confirm that the observed changes, especially the virtual cease of lymph flow from gender-matched grafts at weeks five and ten, were not due to lymph flowing to other lymph nodes not highlighted in the scan, we quantified the loss of radioactivity from the graft (Figure 1m). Indeed, at ten weeks after transplant, four hours after injection of nanocoll, while only 72.1 ± 12.02% of injected radioactivity remains within the graft of HY-mismatched recipients, virtually all (98.7 ± 0.64%) of injected radioactivity has remained within the gender-matched grafts (p = 0.0286), confirming that the rate of lymphatic flow from gender-matched grafts was indeed very low compared with gender-mismatched grafts.

Chronic rejection is associated with myocardial lymphangiogenesis

To determine if changes in LFI were associated with structural changes of lymphatic vessels such as vessel density within donor grafts, vessels were stained with the lymphatic endothelial cell marker LYVE-1 (Figure 2a-c). The number of Myocardial lymphatic vessels increased five-fold with time in the HY-mismatched grafts (Figure 2d; with a mean of 11.75 *vs.* 55 vessels per ten MPF at week one and ten post-transplant, respectively, p=0.038). Subepicardium lymphatic density also increased three-fold in HY-mismatched grafts (Figure 2d; mean of 6.25 *vs.* 18 per ten MPF), suggesting active lymphangiogenesis has occurred during chronic allograft inflammation.

The LYVE-1^{+} Myocardial lymphatic vessel mean area showed an increase at week five compared with week one (Figure 2e) in the HY-mismatched grafts (Mean 252.944μm^2 *vs.* 647.981μm^2, week one and week five, respectively, p=0.0046); which was significantly enhanced in comparison to the gender-matched grafts p<0.0001. However, by week ten the average vessel area is reduced back to levels similar to week one. The subepicardial lymphatic vessel area increased at week ten compared with week one (Figure 2f, mean 207.354μm^2 *vs.* 469.297μm^2, week one and week ten, respectively, p=0.0255); which was significantly enhanced in comparison to the gender-matched grafts p=0.0091.

Lymphatic flow index correlates with lymphatic vessel area, but not density

The higher density of lymphatic vessels within donor grafts has been reported previously, however, this does not necessarily mean higher lymphatic flow or indeed more efficient transport of DPL to dLN. We, therefore, correlated the LFI with the lymphatic vessel density. At week one the enhanced LFI observed in the gender-matched grafts correlated with the myocardial vessel density (Figure 2g, p=0.0021). No correlation was observed between the LFI and lymphatic vessel number in either graft type at the later time points (Table 1). However, as not all vessels have the same diameter, we, therefore, correlated LFI with the mean lymphatic vessel area. Overall, at all time points, the LFI correlated stongly with lymphatic vessel area (Figure 2h-k), except for the subepicardium area in the HY-mismatch at week five (Figure 2j). At week one, in both graft types, enhanced myocardial

lymphatic vessel area correlated with the LFI (Figure 2h, HY-mismatch p=0.0008 & Gender-matched p=0.0003); this was also the case for the subepicardial vessel area in the gender-matched grafts (Figure 2i, p=0.008). However, in the HY-mismatched grafts, the reduced LFI inversely correlated with enhanced subepicardial vessel area (Figure 2i, p<0.0001). The enhanced LFI and myocardial vessel area both observed in the HY-mismatch grafts at week five, resulted in the most statistically significant correlation (Figure 2j, p<0.0001, R^2=0.9861, r_s=1), which was not observed in the gender-matched grafts. No correlation was observed for the subepicardium area in the HY-mismatch at week five (Figure 2j). At ten weeks' post-transplant in recipients of an HY-mismatch cardiac graft, the LFI did positively correlate with an increase in the mean myocardial and subepicardial lymphatic vessel area (Figure 2k, HY-mismatch p=0.0222 & Gender-matched p=0.0222). Suggesting that at the later time points it is increased area, not the number of vessels that allows an increased flow out of the graft.

Donor cells are the main source of neo-lymphangiogenesis in cardiac allografts

In fully MHC-mismatched transplantation models, lymphatic vessels are a combination of donor and recipient-derived11. To determine if changes in LFI was due to lymphangiogenesis of donor or recipient lymphatic vessels, donor hearts were stained for expression of EYFP, expressed only by the recipient. Co-localization of EYFP and LYVE-1 in sections obtained ten weeks after surgery demonstrated that the vast majority of lymphatic vessels were donor derived (Figure 2l-s $YFP^-/LYVE\text{-}1^+$), with only occasional recipient-derived ($YFP^+/LYVE\text{-}1^+$) lymphatic vessels (Figure 2t-w). On quantification, the average recipient *de novo* lymphatic vessel area was 144.72+17.7μm^2. This is smaller in comparison to the average myocardial vessel area observed at week one of 252.944μm^2 and the subepicardial lymphatic vessel area of 207.354μm^2, however, this is consistent with newly forming vessels.

Lymphatic flow index correlates with trafficking of donor cells to draining lymph nodes

Migration of DPL out of donor organs to dLN is a key early event in the initiation of the immune response. To determine the number of donor cells that have migrated out of the grafts we isolated genomic DNA from the mediastinal dLN to quantify the number of male donor cells present after transplantation using a standard curve generated by real-time PCR (Figure 3a). One-week post-transplant, 1708 ± 1324 male donor cells (Figure 3b, p = 0.0019); being 0.12 ± 0.07% of the recipient cells (Figure 3c p = 0.0019) were detected in the mdLN following transplantation. The percentage of male donor cells present in dLN of recipients strongly correlated with LFI (Figure 3d & Table 2; p<0.0001, r_s= 1); as well as the number of $CD8^+$ cells within the donor graft in the same recipients (Figure 3e & Table 2; p=0.0081, r_s = 1), suggesting that higher lymphatic flow rate does facilitate trafficking of DPL and the subsequent immune response.

Cardiac Allograft Vasculopathy correlates with increased lymphatic vessel area and infiltrating $CD8^+$ T-cells

As the LFI correlates with trafficking of donor cells to dLN, and we have demonstrated previously DPL elicit a donor-specific $CD8^+$ T-cell response in the mdLN8; we hypothesized that initial variation in LFI from donor grafts to the mdLN could alter the

subsequent priming of the immune response and thus cellular infiltration into the graft and this, in turn, would lead to graft vasculopahty. Over the time course, the number of $CD4^+$ (Figure 4a & 4d), $CD8^+$ (Figure 4b & 4e) and $CD68^+$ (Figure 4c & 4f) cells increased in the grafts of HY-mismatched recipients. At the earlier time points, small numbers of $CD4^+$, $CD8^+$, and $CD68^+$ cells were seen in the gender-matched grafts however, inflammation had resolved after five weeks (Figure 4). In the HY-mismatched graft at week five $CD68^+$ macrophages were the predominant infiltrating cell population (Figure 4g), which mirrors the HY-mismatched LFI (Figure 1l) and myocardial vessel area (Figure 2e & Figure 2j). The percentage of $CD8^+$ cells increased over time in the HY-mismatched graft (Figure 4g) and was consistently higher than the gender-matched graft (Figure 4h). Cellular infiltration was reflected in graft damage as evident by the development of CAV, determined by vessel luminal occlusion (Figure 4i-k), which increased in the transplanted graft over time (Figure 4l, $p<0.0001$). There was a strong correlation between CAV, and the number of $CD8^+$ T-cells within the HY-mismatched grafts (Figure 4m, Table 3; $p<0.0001$, $r_s=1$) as well as the mean lymphatic vessel area (Figure 4n, $p<0.0001$,Table 3; $r_s=1$).

The lymphatic flow index and increased lymphatic vessel area correlate with inflammatory infiltrate in cardiac grafts

Differences in lymphatic flow from donor grafts are likely to have an influence on the inflammatory response. Likewise, the severity of the inflammatory response may also affect lymphangiogenesis and lymphatic flow. We, therefore, correlated LFI and lymphatic vessel area with inflammatory infiltrates within the donor grafts. Results are summarised in Table 4. Overall, with HY-mismatch grafts, enhanced LFI and increased lymphatic area, respectively, correlated with enhanced $CD8^+$ T-cell infiltration at week one (Figure 4o, $p=0.0008$ & Figure 4p, *$p<0.0001$*); and at week 10 (Figure 4q, $p=0.0218$ & Figure 4r, myocardium $p=0.0060$, subepicardium $p=0.0004$). Enhanced $CD4^+$ T-cell infiltration also correlated with increased lymphatic area in HY-mismatched grafts, in the subepicardium at week one (Figure 4s, *$p<0.0001$*) and myocardium at week ten (Figure 4t, $p=0.0206$). Interestingly, there is an inverse correlation with $CD4^+$ T-cells (Figure 4s) and $CD68^+$ macrophages (Figure 4u, $p=0.0016$, $r_s=0.8$) and the myocardial vessel area at week one and the number of $CD68^+$ macrophages at week ten (Figure 4v, myocardium $p<0.0001$, subepicardium $p=0.0008$). This may be due to the early processes of lymphangiogenesis; where macrophages transdifferentiate into lymphatic endothelial cells11 and $CD4^+$ T-cells increase lymphagiogenesis *via* VEGF-A and VEGF-C expression27. Collectively, indicative that the chronic inflammatory environment, in combination with the increased lymphatic vessel area, has allowed increased trafficking to the mdLN, and in turn inflammatory cell recruitment to the graft.

Discussion

Development of cardiac allograft vasculopathy (CAV), is the main limitation of long-term survival of heart transplant patients4. It is hypothesised that CAV is a result of interrupted lymphatic drainage after surgery9. We used SPECT/CT lymphoscintigraphy to provide an objective quantification of lymphatic flow following transplantation and correlated it with the immune response. It is important to note that the parameters measured result in an index,

not an actual quantification of lymphatic flow rate in terms of volume per unit time. Nonetheless, it provides an objective quantification of lymph flow and allows us to compare flow rates between allografts and correlate this with lymphatic density within the donor graft and other immunological events. We have chosen a single minor antigen (HY) mismatched model to allow time for chronic rejection to develop and any changes in lymphatic vessels within the donor graft to take place26. Minor antigens are only recognised by the recipient *via* the indirect pathway of antigen presentation, a route associated with chronic rejection28.

After organ transplantation, donor lymphatics re-connect to the local lymphatic network of the recipient. It is now well established that on transplantation of organs into the abdomen, the donor organ lymphatics connect to the sub-diaphragmatic network of the recipient, which drains to the mediastinal-LN8, 29–32, rather than lymphatic chains more locally, such as the mesenteric chain. The reason for this is unclear. To support this observation, we have previously demonstrated the presence of high numbers of donor-specific T-cells in the mediastinal-LN, but not in irrelevant non-draining LN. Occasionally, mesenteric-LN contain a small population of donor-specific T-cells, but it is not a constant feature8. For orthotropic heart transplant, as in the clinical situation, donor lymphatics will drain to the local-dLN. Although the exact sites may not be well established, the immunological effect should not be the same wherever the donor lymph drains, as the dLNs merely provide a niche for the donor antigens to meet their cognate alloreactive T-cells, which after activation, traffic *via* blood to the donor graft, resulting in rejection.

The key question we set out to address is whether the higher density of lymphatic vessels observed within donor organs after transplantation is associated with enhanced lymphatic flow or more efficient transport of DPL to the dLN; leading to enhanced alloimmunity; i.e. do changes in lymphatic structure result in changes in function?

In our model, there was an increase in lymphatic density, in concordance with other models of cardiac4 and kidney33, 34 mouse and rat transplantation (Figure 2). However, others have shown in human and rat cardiac allografts, a lower density of lymphatics correlated with rejection13, 16, 35. This may be due to differences in timing or location within the graft, for example, in a rat allograft model13 in agreement with our data, a significant increase in vessel density is observed within the inner lymphatics, however, a decrease is observed in the outer lymphatics. Indeed, variations between different models may indicate that determining vessel density by histology alone may not be a reliable indicator of graft rejection.

We found a higher LFI in the gender-matched group compared with the HY-mismatched group at week one (Figure 1); which correlated with enhanced lymphatic vessel number (Figure 2g), as well as, myocardial and subepicardial area (Figure 2h-k). The reason for this is unclear, but lymphatic flow out of the graft in the gender-matched recipients may lead to beneficial effects such as resolving tissue oedema and promoting clearance of inflammatory cells and cytokines to resolve local inflammation32, 36, which does not occur in the HY-mismatch recipients37. At week one enhanced LFI inversely correlated with reduced subepicardial lymphatic vessel area in the HY-mismatched graft (Figure 2i). An oedema,

with enhanced cell and fluid load may well be present due to inflammation in the HY-graft, which results in increased contractile pressure and lymph flow through the smaller vessels.

The increase in LFI in the HY-mismatched donor grafts compared with gender-matched grafts at weeks five and ten (Figure 1) is not surprising, given the number of lymphatic vessels is increased; potentially allowing more flow of lymph out of the grafts. However, the difference between the HY-mismatched and gender-matched grafts was surprising and is disproportionate to the difference in lymphatic vessel density observed between the two groups, suggesting that additional factors, such as the inflammatory milieu within HY-mismatched grafts, may play a role in increasing the lymphatic flow. Furthermore, the LFI correlated with lymphatic vessel area, not density (Figure 2 & Table 1). The low LFI to the mdLN in gender-matched recipients was not due to drainage to a different set of dLN and therefore, was missed by the SPECT/CT scans as evident from the SPECT/CT scans; showing a slow rate of nanocoll leaving the grafts, especially at week ten (Figure1m).

In the HY-mismatch recipients, the myocardial lymphatic vessel area peaked at week five and decreased subsequently (Figure 2e), the percentage of infiltrating $CD68^+$ macrophages corresponded with this (Figure 4g), which also mirrored a peak at weak five in the LFI (Figure 1l & Figure 2j). Indicative that the macrophages may play a role in increasing the vessel area by trans-differentiation and *de novo* lymphangiogenesis11. Lymphatic density increased with time (Figure 2d), however, despite an increase in density at week ten the LFI decreased. In a model of cutaneous hypersensitivity, inflammatory driven lymphatic endothelial cell proliferation and lymphatic remodelling did not affect the lymphatic vessel density, but vessels increased in size affecting lymph flow38. In addition, to physical factors such as vessel area, lymph flow is regulated by complex interactions of phasic, and sustained, tonic contractions of the lymphatic smooth muscles; where force and frequency of lymphatic contraction can be influenced by a variety of signals including cytokines37. Therefore, the active inflammation, and enhanced myocardial lymphatic area, observed in week five, may result in the enhanced lymphatic flow observed here.

Previously we have shown in both abdominal and cervical transplantation, leakage from the open severed ends of the lymphatic vessels drains into mdLN and that intact lymphatic vessels are not essential for flow towards these particular dLN8. By week five the lymphatic vessels have reconnected and we speculate therefore that there is no longer any leak into the peritoneum in the gender-matched recipients. However, in the HY-mismatch recipients, due to the process of inflammatory driven lymphangiogenesis, we observe the lymphatic vessels enlarge (Figure 2e) presumably becoming leaky allowing lymph to continue to traffic to the mdLN.

We found that LFI at the earliest time point (week one) strongly correlated with the percentage of male donor-derived cells determined to be present in the mdLN (Figure 3c). This in turn correlated with increased numbers of $CD8^+$ T-cells within the donor graft (Figure 3e). The number of $CD8^+$ T-cells within the HY-mismatched grafts correlated with the level of CAV, determined by vessel occlusion (Figure 4m). Furthermore, CAV correlated with the mean lymphatic vessel area (Figure 4n). There is also a positive correlation with the increased $CD8^+$ T-cells and LFI at weeks one (Figure 4o) and ten (Figure 4q); and the mean

lymphatic vessel area at weeks one (Figure 4p) and ten (Figure 4r). Increased numbers of $CD4^+$ T-cells also correlated with the lymphatic vessel area in the subepicardium at week one (Figure 4s) and the myocardium at week ten (Figure 4t). Combined, this data supports the notion that increased lymphatic flow is associated with increased trafficking of DPL to dLN, which leads to an enhanced subsequent alloimmune response; which we have shown previously in our model is $CD8^+$ T-cell driven8. In support of this, in a study of human renal transplants34 rejection was caused by a lymphocyte-rich inflammatory infiltrate, attracted by CCL21 produced by lymphatic endothelial cells. The authors speculated that *neo*-lymphangiogenesis contributed to the export of APCs, which in turn induced an alloreactive immune response34. Furthermore, Lakkis *et al.* concluded that the rejection process is dependent on a suitable niche for interactions between APCs and recipient T-cells, with rejection being considerably delayed in mice lacking lymph nodes, and completely halted in alymphoplastic splenectomised recipients39.

The lymphatic vessel area may be enhanced by the previously reported process of B cell-driven lymphangiogenesis40. In our model of CAV, we found evidence that the early process of lymphangiogenesis appears to be due to the numbers of $CD4^+$ T-cells and $CD68^+$ macrophages resident in the graft (Table 4 & Figure 4g, s-v). $CD4^+$ T-cells have been previously shown to increase lymphatic vessels density through increased expression of VEGF-A and VEGF-C27. Furthermore, macrophages have been shown to play a role in *de novo* lymphangiogenesis11.

Our results indicate that most of the lymphatic vessels were of donor rather than recipient origin (Figure 2a-i). This is in concordance with some published data4, 11, but not others41. These differences may be due to the different models used. Kerjaschki *et al.* demonstrated that *de novo* lymphangiogenesis involved incorporation of recipient-derived lymphatic progenitors, derived from infiltrating macrophages11 in human kidney allografts. Our model is a single minor antigen mismatch, which results in only a moderate degree of inflammation, which may not be enough to result in a high proportion of recipient-derived lymphatic vessels.

We attempted to correlate LFI with the anti-donor response, such as graft infiltration at later time points. Overall, positive correlations were found (Tables 1–4 & Figure 4). However, this data must be interpreted with care as LFI and the donor response are clearly interdependent, with each having the potential to enhance the other. Therefore, data presented here do not provide evidence for cause and effect, but nonetheless, provide some insight into the complex interplay between lymphatic function and the inflammatory response.

In conclusion, the LFI provides a functional assessment of lymphatic flow following transplant. Lymph flow is enhanced in HY-mismatched grafts compared with gender matched grafts to a degree that cannot be accounted for by the increased lymphatic vessel density alone, implying that inflammation may enhance the flow of lymph. As ischaemia/reperfusion injury affects lymphatic flow from the heart, and this change is seen before myocardial necrosis is visible. Changes in lymphatic drainage could be an early marker of heart disease and allow for an early diagnosis42, 43. Therefore, SPECT-CT imaging could

Europe PMC Funders Author Manuscripts

prove to be an extremely useful tool in transplantation research and in clinical investigation with the potential to be adapted to detect early heart disease. Despite advances in graft survival rate, there is still a need for targeted suppression of alloimmunity and subsequent eradication of CAV and rejection. The data suggests that interference of lymphatic flow to the mdLN at the time of transplant would promote graft survival. Pre-clinical models using donors with disrupted lymphatics would definitively prove this point. Treatment with inhibitors of lymphatic flow or lymphangiogenesis (e.g. post-harvest using complement fixing anti-LYVE-1 antibodies) could be used as a first step to treat patients who have received a heart transplant as used in other disease models44, 45 and can be adapted for use in transplantation.

Supplementary Material

Refer to Web version on PubMed Central for supplementary material.

Acknowledgements

The authors acknowledge the support of the MRC Centre for Transplantation. The work was performed in collaboration with Drs Greg Mullen and Kavitha Sunassee in the Division of Imaging Sciences, King's College London. The ROSA-EYFP mice were a kind gift from Professor Anthony Dorling.

Funding Sources

This work was funded by the British Heart Foundation grant number: PG/13/29/30121 and an MRC centre grant (MR/J006742/1). The SPECT/CT scanner used was funded by a grant from the Wellcome Trust.

Reference List

(1). Taylor R, Lannon J, Wong E, Collett D. Annual Report on Cardiothoracic Transplantation. Statistics & Clinical Studies, NHS Blood & Transplant. 2015:1–131. http://www.odt.nhs.uk/pdf/organ_specific_report_cardiothoracic_2015.pdf.

(2). Sayegh MH, Carpenter CB. Transplantation 50 years later--progress, challenges, and promises. N Engl J Med. 2004; 23:2761–6.

(3). Lund LH, Edwards LB, Kucheryavaya AY, Benden C, Christie JD, Dipchand AI, Dobbels F, Goldfarb SB, Levvey BJ, Meiser B, Yusen RD, et al. The Registry of the International Society for Heart and Lung Transplantation: Thirty-first Official Adult Heart Transplant Report 2014; Focus Theme: Retransplantation. The Journal of Heart and Lung Transplantation. 2014; 33:996–1008. [PubMed: 25242124]

(4). Nykanen AI, Sandelin H, Krebs R, Keranen MA, Tuuminen R, Karpanen T, Wu Y, Pytowski B, Koskinen PK, Yla-Herttuala S, Alitalo K, et al. Targeting lymphatic vessel activation and CCL21 production by vascular endothelial growth factor receptor-3 inhibition has novel immunomodulatory and antiarteriosclerotic effects in cardiac allografts. Circulation. 2010; 121:1413–22. [PubMed: 20231530]

(5). Hasegawa T, Visovatti SH, Hyman MC, Hayasaki T, Pinsky DJ. Heterotopic vascularized murine cardiac transplantation to study graft arteriopathy. Nat Protoc. 2007; 2:471–80. [PubMed: 17406609]

(6). Beland S, Desy O, Vallin P, Basoni C, De Serres SA. Innate immunity in solid organ transplantation: an update and therapeutic opportunities. Expert Rev Clin Immunol. 2015; 11:377–89. [PubMed: 25644774]

(7). Ochando JC, Homma C, Yang Y, Hidalgo A, Garin A, Tacke F, Angeli V, Li Y, Boros P, Ding Y, Jessberger R, et al. Alloantigen-presenting plasmacytoid dendritic cells mediate tolerance to vascularized grafts. Nat Immunol. 2006; 7:652–62. [PubMed: 16633346]

(8). Brown K, Badar A, Sunassee K, Fernandes MA, Shariff H, Jurcevic S, Blower PJ, Sacks SH, Mullen GE, Wong W. SPECT/CT lymphoscintigraphy of heterotopic cardiac grafts reveals novel sites of lymphatic drainage and T cell priming. Am J Transplant. 2011; 11:225–34. [PubMed: 21219574]

(9). Miller AJ, DeBoer A, Palmer A. The role of the lymphatic system in coronary atherosclerosis. Med Hypotheses. 1992; 37:31–6. [PubMed: 1569904]

(10). Vass DG, Hughes J, Marson LP. Restorative and rejection-associated lymphangiogenesis after renal transplantation: friend or foe? Transplantation. 2009; 15:1237–9.

(11). Kerjaschki D, Huttary N, Raab I, Regele H, Bojarski-Nagy K, Bartel G, Krober SM, Greinix H, Rosenmaier A, Karlhofe F, Wick N, et al. Lymphatic endothelial progenitor cells contribute to de novo lymphangiogenesis in human renal transplants. Nat Med. 2006; 12:230–4. [PubMed: 16415878]

(12). Maruyama K, Ii M, Cursiefen C, Jackson DG, Keino H, Tomita M, Van Rooijen N, Takenaka H, D'Amore PA, Stein-Streilein J, Losordo DW, et al. Inflammation-induced lymphangiogenesis in the cornea arises from CD11b-positive macrophages. J Clin Invest. 2005; 115:2363–72. [PubMed: 16138190]

(13). Soong TR, Pathak AP, Asano H, Fox-Talbot K, Baldwin WM III. Lymphatic injury and regeneration in cardiac allografts. Transplantation. 2010; 89:500–8. [PubMed: 20118845]

(14). Di CE, D'Antuono T, Contento S, Di NM, Ballone E, Sorrentino C. Quilty effect has the features of lymphoid neogenesis and shares CXCL13-CXCR5 pathway with recurrent acute cardiac rejections. Am J Transplant. 2007; 7:201–10. [PubMed: 17061985]

(15). Jonigk D, Lehmann U, Stuht S, Wilhelmi M, Haverich A, Kreipe H, Mengel M. Recipient-derived neoangiogenesis of arterioles and lymphatics in quilty lesions of cardiac allografts. Transplantation. 2007; 84:1335–42. [PubMed: 18049119]

(16). Geissler HJ, Dashkevich A, Fischer UM, Fries JW, Kuhn-Regnier F, Addicks K, Mehlhorn U, Bloch W. First year changes of myocardial lymphatic endothelial markers in heart transplant recipients. Eur J Cardiothorac Surg. 2006; 29:767–71. [PubMed: 16439147]

(17). Jones D, Min W. An overview of lymphatic vessels and their emerging role in cardiovascular disease. J Cardiovasc Dis Res. 2011; 2:141–52. [PubMed: 22022141]

(18). de Boer J, Williams A, Skavdis G, Harker N, Coles M, Tolaini M, Norton T, Williams K, Roderick K, Potocnik AJ, Kioussis D. Transgenic mice with hematopoietic and lymphoid specific expression of Cre. Eur J Immunol. 2003; 33:314–25. [PubMed: 12548562]

(19). Srinivas S, Watanabe T, Lin CS, William CM, Tanabe Y, Jessell TM, Costantini F. Cre reporter strains produced by targeted insertion of EYFP and ECFP into the ROSA26 locus. BMC Dev Biol. 2001; 1:4. [PubMed: 11299042]

(20). Corry RJ, Winn HJ, Russell PS. Primarily vascularized allografts of hearts in mice. The role of H-2D, H-2K, and non-H-2 antigens in rejection. Transplantation. 1973; 16:343–50. [PubMed: 4583148]

(21). Wong W, Morris PJ, Wood KJ. Pretransplant administration of a single donor class I major histocompatibility complex molecule is sufficient for the indefinite survival of fully allogeneic cardiac allografts: evidence for linked epitope suppression. Transplantation. 1997; 63:1490–4. [PubMed: 9175815]

(22). Superina RA, Peugh WN, Wood KJ, Morris PJ. Assessment of primarily vascularized cardiac allografts in mice. Transplantation. 1986; 42:226–7. [PubMed: 3526662]

(23). Tapmeier TT, Fearn A, Brown K, Chowdhury P, Sacks SH, Sheerin NS, Wong W. Pivotal role of CD4+ T cells in renal fibrosis following ureteric obstruction. Kidney Int. 2010; 78:351–62. [PubMed: 20555323]

(24). An N, Kang Y. Using quantitative real-time PCR to determine donor cell engraftment in a competitive murine bone marrow transplantation model. J Vis Exp. 2013; 73:e50193.

(25). Byrne P, Huang W, Wallace VM, Shean MK, Zhang Z, Zhong Q, Theodossiou C, Blakesley H, Kolls JK, Schwarzenberger P. Chimerism analysis in sex-mismatched murine transplantation using quantitative real-time PCR. Biotechniques. 2002; 32:279–4. [PubMed: 11848403]

(26). He C, Schenk S, Zhang Q, Valujskikh A, Bayer J, Fairchild RL, Heeger PS. Effects of T cell frequency and graft size on transplant outcome in mice. J Immunol. 2004; 172:240–7. [PubMed: 14688331]

(27). Zampell JC, Yan A, Elhadad S, Avraham T, Weitman E, Mehrara BJ. CD4(+) cells regulate fibrosis and lymphangiogenesis in response to lymphatic fluid stasis. PLoS One. 2012; 7:e49940. [PubMed: 23185491]

(28). Afzali B, Lombardi G, Lechler RI. Pathways of major histocompatibility complex allorecognition. Curr Opin Organ Transplant. 2008; 13:438–44. [PubMed: 18685342]

(29). Sicard A, Phares TW, Yu H, Fan R, Baldwin WM, Fairchild RL, Valujskikh A. The Spleen is the Major Source of Anti-Donor Antibody Secreting Cells in Murine Heart Allograft Recipients. Am J Transplant. 2012; 12:1708–19. [PubMed: 22420367]

(30). Olin T, Saldeen T. The Lymphatic Pathways from the peritoneal cavity: A Lymphangiographic study in the rat. Cancer Res. 1964; 24:1700–11. [PubMed: 14230917]

(31). Bennett HS, Shivas AA. The visualization of lymph-nodes and vessels by ethyl iodostearate (angiopac) and its effect on lymphoid tissue; a preliminary radiological and histological study. J Fac Radiol. 1954; 5:261–6. [PubMed: 24543589]

(32). Cui Y. The role of lymphatic vessels in the heart. Pathophysiology. 2010; 17:307–14. [PubMed: 19942415]

(33). Brown K, Sacks SH, Wong W. Tertiary lymphoid organs in renal allografts can be associated with donor-specific tolerance rather than rejection. Eur J Immunol. 2011; 41:89–96. [PubMed: 21182080]

(34). Kerjaschki D. Lymphatic neoangiogenesis in renal transplants: a driving force of chronic rejection? J Nephrol. 2006; 19:403–6. [PubMed: 17048196]

(35). Ruggiero R, Muz J, Fietsam R Jr, Thomas GA, Welsh RJ, Miller JE, Stephenson LW, Baciewicz FA Jr. Reestablishment of lymphatic drainage after canine lung transplantation. J Thorac Cardiovasc Surg. 1993; 106:167–71. [PubMed: 8320995]

(36). Kim H, Kataru RP, Koh GY. Inflammation-associated lymphangiogenesis: a double-edged sword? J Clin Invest. 2014; 124:936–42. [PubMed: 24590279]

(37). Al-Kofahi M, Becker F, Gavins FN, Woolard MD, Tsunoda I, Wang Y, Ostanin D, Zawieja DC, Muthuchamy M, von der Weid PY, Alexander JS. IL-1beta reduces tonic contraction of mesenteric lymphatic muscle cells, with the involvement of cycloxygenase-2 and prostaglandin E2. Br J Pharmacol. 2015; 172:4038–51. [PubMed: 25989136]

(38). Lachance PA, Hazen A, Sevick-Muraca EM. Lymphatic vascular response to acute inflammation. PLoS One. 2013; 8:e76078. [PubMed: 24086691]

(39). Lakkis FG, Arakelov A, Konieczny BT, Inoue Y. Immunologic 'ignorance' of vascularized organ transplants in the absence of secondary lymphoid tissue. Nat Med. 2000; 6:686–8. [PubMed: 10835686]

(40). Angeli V, Ginhoux F, Llodra J, Quemeneur L, Frenette PS, Skobe M, Jessberger R, Merad M, Randolph GJ. B cell-driven lymphangiogenesis in inflamed lymph nodes enhances dendritic cell mobilization. Immunity. 2006; 24:203–15. [PubMed: 16473832]

(41). Yan A, Avraham T, Zampell JC, Aschen SZ, Mehrara BJ. Mechanisms of Lymphatic Regeneration after Tissue Transfer. PLoS One. 2011; 6:e17201. [PubMed: 21359148]

(42). Santos AC, de Lima JJ, Botelho MF, Pacheco MF, Sousa P, Bernardo J, Ferreira N, Goncalves L, Aguiar J, Providencia LA, Pauwels EK. Cardiac lymphatic dynamics after ischemia and reperfusion--experimental model. Nucl Med Biol. 1998; 25:685–8. [PubMed: 9804050]

(43). Szlavy L, Koster K, de Court, Hollenberg NK. Early disappearance of lymphatics draining ischemic myocardium in the dog. Angiology. 1987; 38:73–84. [PubMed: 3813124]

(44). Wong W, Fry J, Hyde K, Stranford S, Morris PJ, Wood KJ. Haematopoietic stem cells transduced with a single donor class I major histocompatibility complex gene can induce operational tolerance to fully allogeneic cardiac allografts. Transplant Proc. 1999; 31:886. [PubMed: 10083388]

(45). Wong, W., Fry, J., Hyde, K., Morris, PJ., Wood, KJ. Gene transfer and tolerance induction. Microsurgical models in rats and mice for transplantation research. Timmermann, W.Gassel, H-J.Ulrichs, K.Zhong, R., Thiede, A., editors. Springer-Verlag; Berlin: 1998. p. 299-312.

Europe PMC Funders Author Manuscripts

Clinical Perspective

What is new?

- Up to 10–12% of cardiac transplant recipients develop cardiac allograft vasculopathy (CAV) each year, making CAV the leading cause of death in patients more than 5 years' post-transplantation.
- It is hypothesised that CAV results due to interrupted lymphatic drainage post-surgery.
- Despite this, the lymphatic network of the heart and its role in transplant rejection has been largely neglected.
- In this study, we used SPECT/CT lymphoscintigraphy in a pre-clinical model providing an objective quantification of lymphatic flow following transplantation that could be correlated to CAV; demonstrating that cardiac lymphatic remodelling and lymphatic transport dysfunction, post-transplant is associated with CAV and transplant rejection.

What are the clinical implications?

- Despite advances in graft survival, there is still a real need for targeted eradication of CAV.
- Our findings indicate that lymphatic flow is increased during chronic rejection. This, in turn, may result in enhanced trafficking of antigen presenting cells to the local draining lymph nodes and an augmented alloimmune response.
- Although the cause and effect of this phenomenon are yet to be fully established, our data provide the impetus for the investigation of lymphangiogenesis inhibition as a means to dampen chronic rejection.

Europe PMC Funders Author Manuscripts

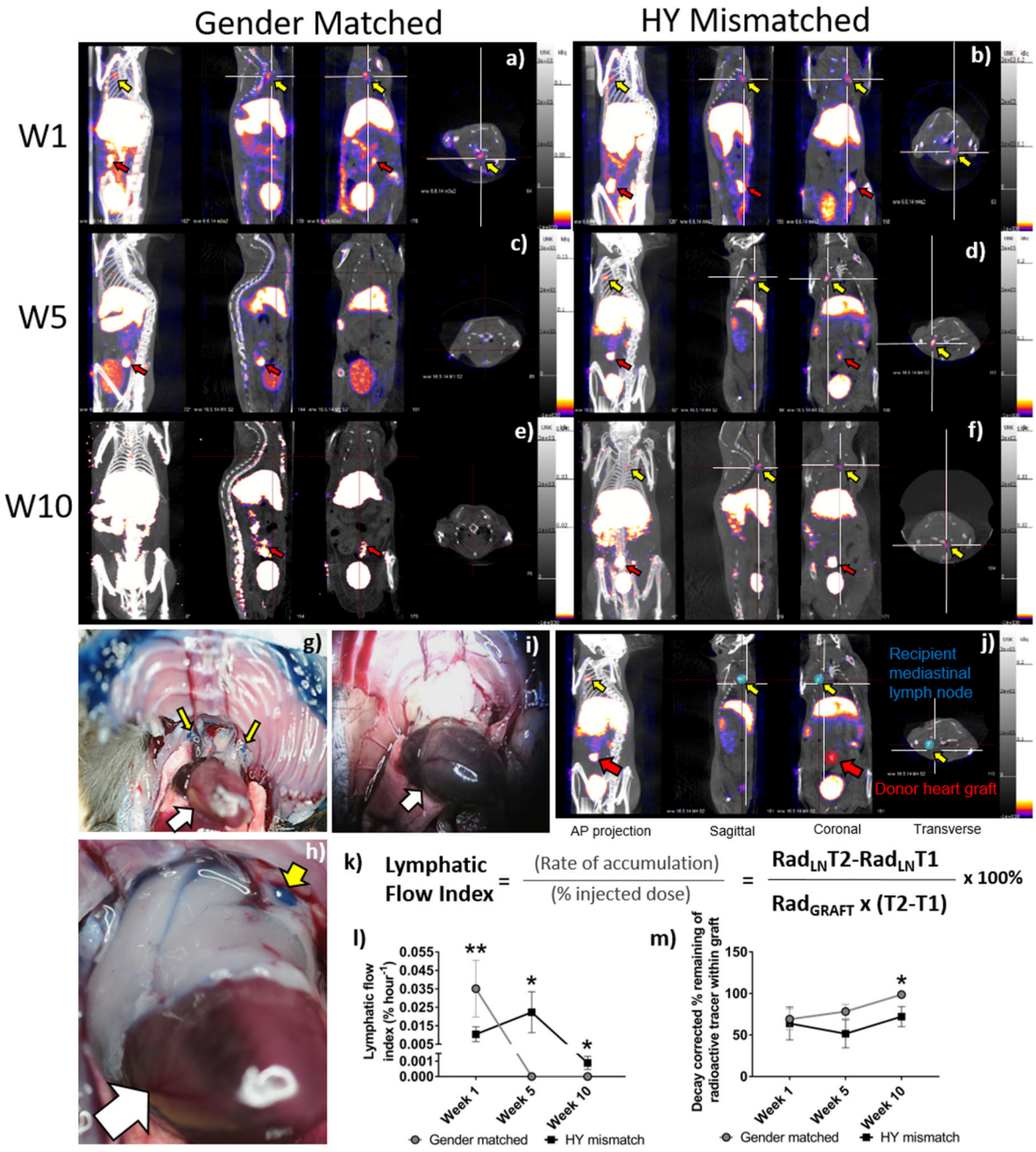

Figure 1. Quantification of the Lymphatic Flow Index from the cardiac grafts to the mediastinal lymph nodes.

SPECT/CT images were taken after injection of nanocoll into the apex of transplanted hearts. Representative images are shown (n = 4-5 per group) in four planes the anterior-posterior view, sagittal, coronal and transverse taken at the same point of the “crosshairs” (white). One (a-b), five (c-d) or ten (e-f) weeks after either gender-matched (a, c & e) or HY-mismatched (b, d & f) abdominal heart transplantation, the animal was scanned 30 min and four hours after nanocoll injection. Images are shown at four-hours post-injection. Representative examples of direct visualisation of lymph drainage from donor heart grafts

after transplantation using Evan's Blue injection (n=3 in each group). Recipient of HY-mismatched donor graft showing mdLN, above the native heart (white arrows), staining blue with Evan's Blue dye (g & h, yellow arrows). Recipient of gender-matched donor graft showing mediastinal not staining blue (i). A sphere is drawn around each “region of interest” (j; blue & red sphere) and the radioactivity quantified in the mdLN (j; Yellow arrow; Rad_{LN}) and the transplanted donor cardiac graft (j; Red arrow; Rad_{graft}). Decay corrected values are used to quantify the lymphatic flow index with T1 being the time of the first scan and T2 being the time of the second scan (k). Shown here is the mean ± SEM, of four to five animals at each time point, of the lymphatic flow index (l) or the percentage loss of injected radiation from the graft (m); with gender-matched and HY-mismatched grafts at weeks, one, five and ten (W1**$p = 0.0080$, W5*$p = 0.0286$ & W10*$p = 0.0156$).

Europe PMC Funders Author Manuscripts

Europe PMC Funders Author Manuscripts

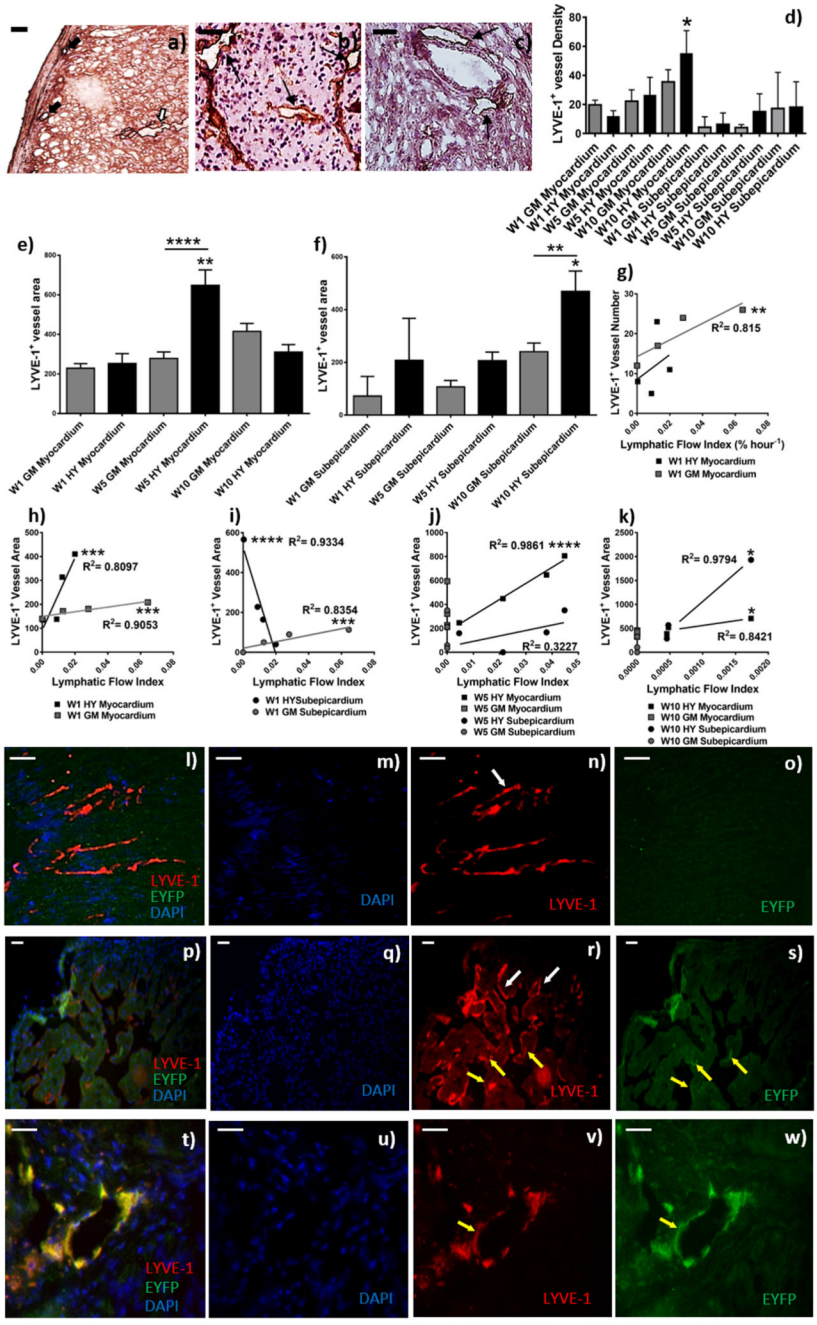

Figure 2. Quantification of lymphatic density in cardiac donor grafts and determination of the origin of LYVE-1$^+$ lymphatic vessels; Lymphatic flow index correlates with lymphatic vessel area, but not density.

After SPECT/CT scanning donor grafts were harvested and used for immunofluorescence and immunohistochemistry. Images are representative examples of four independent experiments; scale bars = 50 μm. Immunohistochemical staining for LYVE-1 was conducted in order to quantify the density of subepicardial (a, the black arrows) and myocardial (a, the white arrows) lymphatic vessels. Shown is a representative of gender-matched (b) and HY-mismatched grafts (c) at ten-weeks post-transplant. The black arrows show LYVE-1$^+$ vessels

(magnification 200x). LYVE-1$^+$ vessels density (d, *p=0.038) and myocardial (e, ****p <0.0001) and subepicardial (f, *p = 0.0091) area (μm^2) was determined by two independent observers in at least 10 medium power fields, with area determined with Image J software. Data are shown as a mean of the two independent observations and four independent experiments ± SEM; of gender-matched (GM) and HY-mismatched (HY) grafts at weeks, one, five and ten. The lymphatic flow index from each individual mouse was correlated with the corresponding LYVE-1$^+$vessel number (g, *p=0.0021) and area at week one (h, Myocardium, HY ***p=0.0008, GM ***p=0.0003; i, subepicardium, HY ****p = 0.0008, GM ***p=0.0003), week five (j, ****p <0.0001) and week ten (k, *p=0.0222). To determine if vessels were of the donor or recipient origin, immunofluorescence was performed with anti-LYVE-1 and anti-YFP. Donor lymphatic vessels are EYFP$^-$ and LYVE-1$^+$(l-s; white arrows). However, the transplant recipients express EYFP and thus recipient lymphatic vessels are EYFP$^+$ and LYVE-1$^+$(t-w; yellow arrows). Shown are a representative of lymphatic vessel staining in gender-matched grafts (l-o) and HY-mismatched grafts (p-s) ten-weeks post-transplant. A representative high power image showing a recipient lymphatic vessel within a donor organ is shown (t-w).

Europe PMC Funders Author Manuscripts

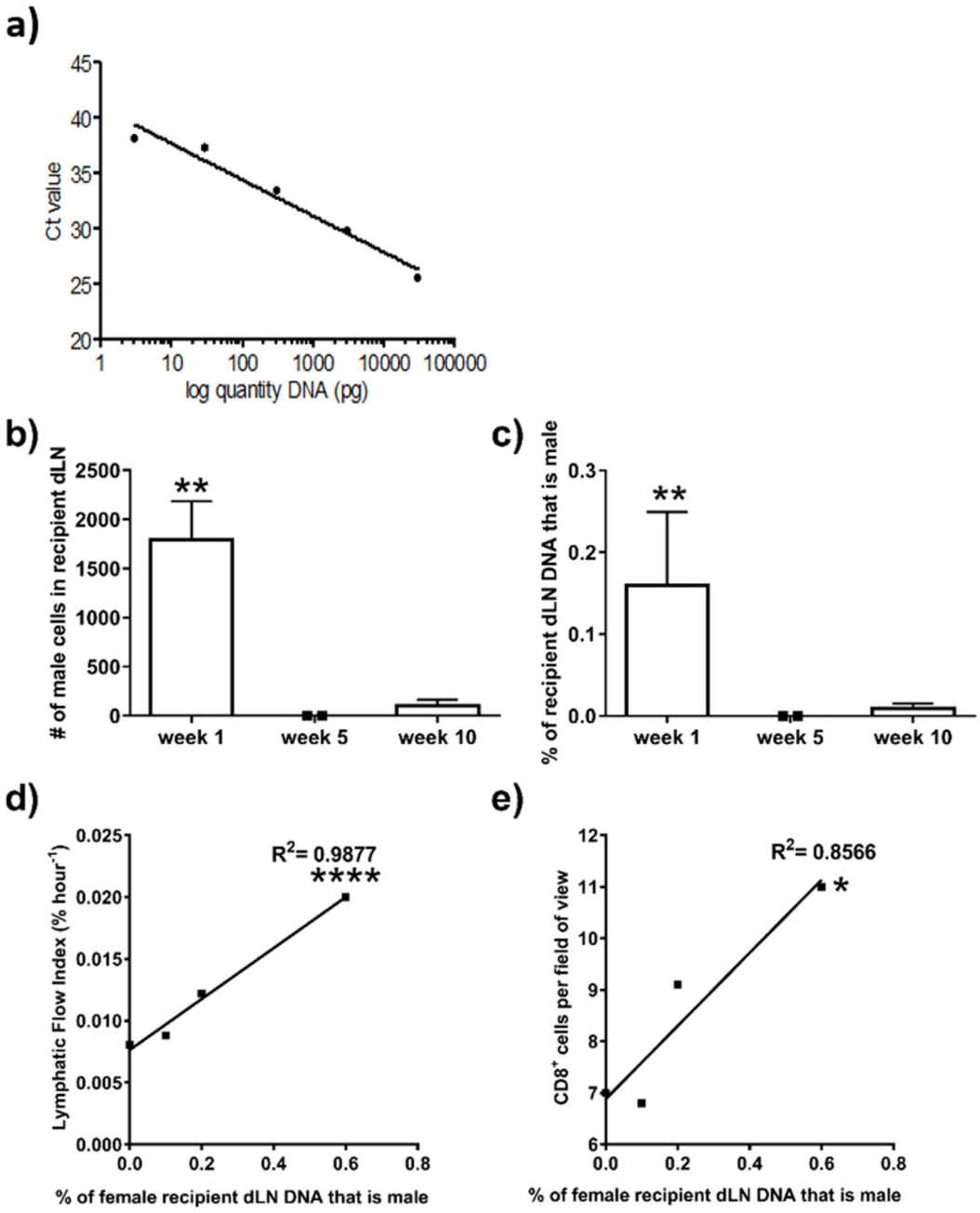

Figure 3. QPCR for donor cells in draining lymph nodes of transplant recipients.

After SPECT/CT imaging, the mdLN were harvested. Genomic DNA was isolated and the Y-chromosome specific gene, Zfy1, was amplified using quantitative Real-time PCR. The presence of male donor-derived DNA in the female recipient lymph nodes at week one, five and ten post-transplant was calculated against a standard curve (a) with a known percentage of male DNA, which corresponds to a known number of cells. Allowing for quantification of the number of male donor-derived cells (b, $^{**}p = 0.0019$) as a percentage (c, $^{**}p = 0.0019$) of the total number of cells within the female lymph node. Shown is the mean ±SD of seven

mice. The percentage of male cells present in the draining mediastinal lymph nodes at week one post-transplant from each individual mouse was correlated with the corresponding lymphatic flow index (d, ****p <0.0001) and the number of $CD8^+$ cells (e, *p = 0.0081) within the donor graft at week one; the number of $CD4^+$ cells; $CD68^+$ cells; the number of vessels and the area of vessels within the donor graft at week one.

Europe PMC Funders Author Manuscripts

Europe PMC Funders Author Manuscripts

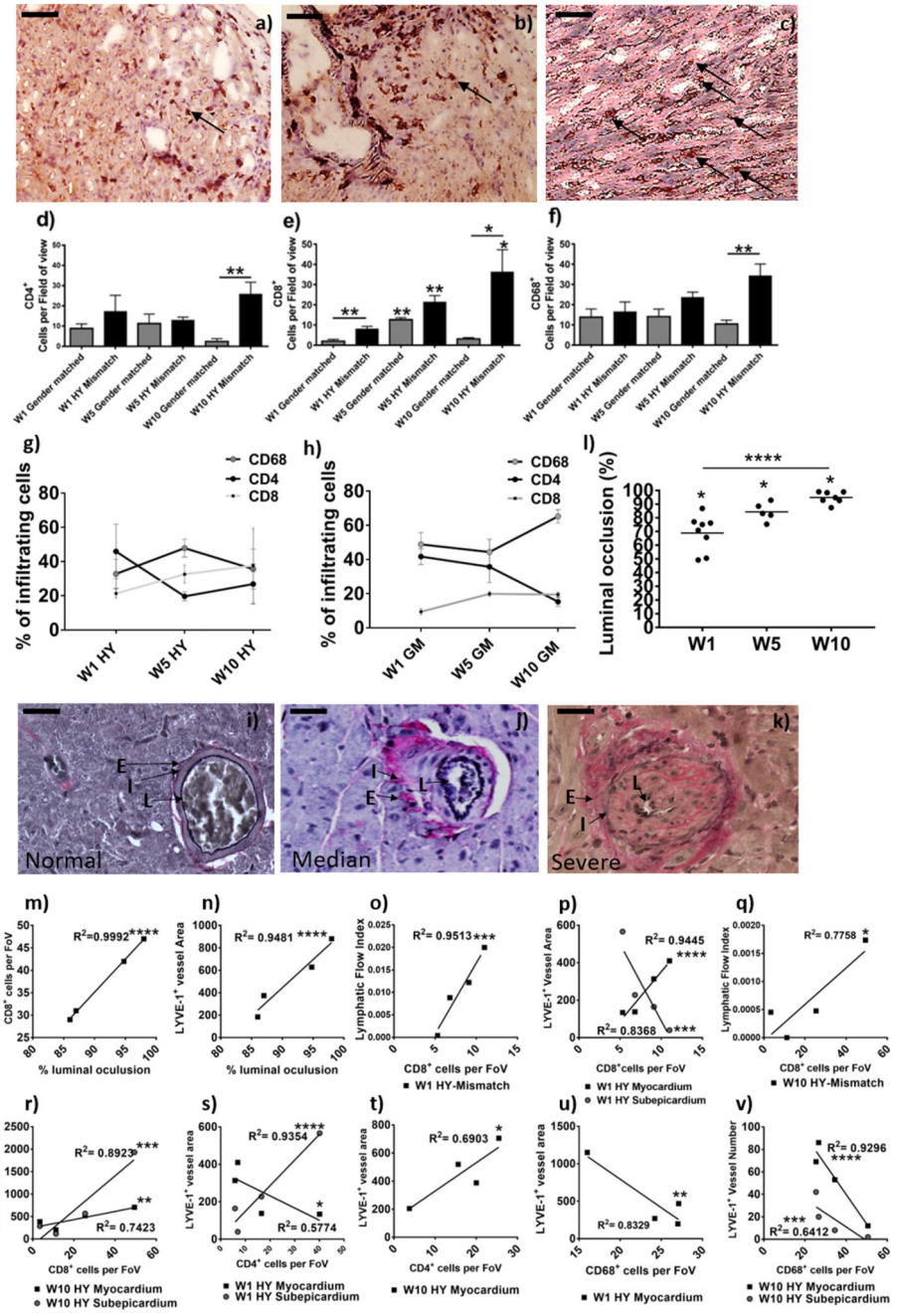

Figure 4. Determination of graft vasculopathy and inflammatory cellular infiltration within the transplanted donor grafts.

After SPECT/CT scanning donor grafts were harvested, immunohistochemical staining for CD4 (a) CD8 (b), and CD68 (c) were conducted to determine cell numbers (black arrows show an example); shown is a representative of HY-mismatched grafts at ten weeks post-transplant. Images are representative examples of 4 independent experiments; scale bars = 50 μm. Positive CD4 (d, $^{**}p = 0.0079$) and CD8 (e, W5GM$^{**}p = 0.0019$, W5HY$^{**}p = 0.0066$, W10HY$^{**}p = 0.0429$, W1GM *vs.* HY$^{**}p = 0.0077$, W10GM *vs.* HY$^{*}p = 0.0233$) cells were counted in 20 random high-power fields (magnification 400x) by two independent

observers. For $CD68^+$ macrophage staining (f, W10**p = 0.0079), a 63-point grid was overlaid onto a 400x magnification of macrophage staining. The percentages of grid points positive for CD68 staining were counted by two independent observers. Data are shown as the mean number of cells, per field of view (FoV), of the two independent observations and four independent experiments ± SEM; of a gender-matched and HY-mismatched grafts at weeks, one, five and ten. Within the infiltrating cells, the percentage of $CD68^+$, $CD4^+$ and $CD8^+$ cells was determined in the HY-mismatched (g) and gender-matched grafts (h). Immunohistochemical staining for Elastic Van Gieson was performed to determine graft vasculopathy. Shown is a representative of a gender-matched (i) and HY-mismatched grafts (j & k). Histologically the allograft vasculopathy ranged from median (j) to severe (k) in the HY mismatched graft. Characterised by inflammatory cell invasion into the layers of the internal to external elastic; shown is the lumen of the vessel (*L*), the internal elastic (*I*) and the external elastic (*E*). Measurement of the internal elastic (*I*) and the external elastic (*E*) can be used to calculate the percentage of luminal occlusion (l, W1*p=0.0121, W5*p=0.0357 & W10*p=0.0238; ****p<0.0001). Shown is the percentage luminal occlusion in four independent experiments with mean at one, five and ten weeks. The percentage luminal occlusion was correlated with $CD8^+$ cell number (m, ****p<0.0001) and the mean lymphatic vessel area (n, ****p<0.0001). $CD8^+$ cell number was correlated with the LFI (o, W1****p<0.0001 & q, W10*p=0.0218) and the lymphatic vessel area (p, myocardial W1****p<0.0001, subepicardial W1***p=0.0008 & r, myocardial W10**p=0.006, subepicardial W10***p=0.0004). $CD4^+$ cell number was correlated with the lymphatic vessel area (s, myocardial W1*p=0.0287 & subepicardial W1****p<0.0001 & t, W10*p=0.0206). $CD68^+$ cell number was correlated with the lymphatic vessel area (u, W1**p=0.0016) and density (v, myocardial W10****p<0.0001 & subepicardial W10***p=0.0008).

Europe PMC Funders Author Manuscripts

Europe PMC Funders Author Manuscripts

Table 1

Correlation of the Lymphatic Flow Index (LFI) to the mediastinal dLN with lymphatic vessel density within the donor graft.

Time point		**Week 1**		**Week 5**		**Week 10**	
Graft Type		**HY Mismatch**	**Gender Matched**	**HY Mismatch**	**Gender Matched**	**HY Mismatch**	**Gender Matched**
Correlation							
LFI *vs.* Myocardial Lymphatic Vessel number	***p***	0.4404	**0.0008** ***	**0.6789**	N/A	**0.0325***	N/A
	R^2	0.1021	**0.815**	**0.03056**		**0.7208**	
	r_s	0.6	**1**	**-0.2**		**-0.5**	
LFI *vs.* *Subepicardial* Lymphatic Vessel number	***p***	0.3849	0.0476	0.7167	N/A	**0.0222***	N/A
	R^2	0.02915	0.01442	0.01442		**0.6084**	
	r_s	-0.4	0.7379	0.2		**-1**	
LFI *vs.* Myocardial Lymphatic Vessel Area	***p***	**0.0008** ***	**0.0003** ***	**<0.0001** ****	N/A	**0.0222***	N/A
	R^2	**0.8097**	**0.9053**	**0.9861**		**0.8421**	
	r_s	**1**	**1**	**1**		**1**	
LFI *vs.* Subepicardial Lymphatic Vessel Area	***p***	**0.0008** ***	**0.0008** ***	0.1418	N/A	**0.0222***	N/A
	R^2	**0.9334**	0.8354	0.3227		**0.9794**	
	r_s	**-1**	1	0.8		**1**	

R^2- using linear regression analyses; **r_s**- Spearman rank correlation coefficient;

p- probability calculated by spearman rank correlation

(* P ≤ 0.05 ** P ≤ 0.01 *** P ≤ 0.001 **** P ≤ 0.0001)

Table 2

Correlation of the percentage of male donor cells in draining lymph nodes (dLN) with Lymphatic flow index, inflammatory cell infiltrate or lymphatic vessel density.

Correlation		Lymphatic Flow Index	Number $CD4^+$ cells in graft	Number $CD8^+$ cells in graft	Number $CD68^+$ cells in graft	Number of $LYVE\text{-}1^+$ lymphatic vessels	Area of $LYVE\text{-}1^+$ lymphatic vessels
% dLN DNA that is male *vs.*	***p***	**<0.0001 ******	0.2264	**0.0081***	0.3711	0.3711	0.2005
	R^2	**0.9877**	0.3377	**0.8566**	0.02021	0.2021	0.3632
	r_s	**1**	-0.5	**1**	0.5	0.5	-0.5

R^2- using linear regression analyses; **r_S-** Spearman rank correlation coefficient;

***p*-** probability calculated by spearman rank correlation

(* P ≤ 0.05 ** P ≤ 0.01 *** P ≤ 0.001 **** P ≤ 0.0001)

Europe PMC Funders Author Manuscripts

Table 3

Correlation of Chronic Allograft Vasculopathy (CAV) with the number CD8$^+$ cells in donor graft or Area of LYVE-1$^+$ lymphatic vessels within the donor graft.

Correlation		Number CD8$^+$ cells in graft		Area of LYVE-1$^+$ lymphatic vessels	
Graft Type		**HY Mismatch**	**Gender Matched**	**HY Mismatch**	**Gender Matched**
Chronic Allograft Vasculopathy (CAV) *vs.*	***p***	**<0.0001******	0.8411	**0.0002*****	0.365
	R^2	**0.9999**	0.01131	**0.9758**	0.7052
	r_s	**1**	0.5	**1**	1

R^2- using linear regression analyses; **r_s-** Spearman rank correlation coefficient;

***p*-** probability calculated by spearman rank correlation

(* P ≤ 0.05 ** P ≤ 0.01 *** P ≤ 0.001 **** P ≤ 0.0001)

Table 4

Correlation of the Lymphatic Flow Index (LFI) to the mediastinal dLN with inflammatory cell infiltrate within the donor graft.

Time point		Week 1		Week 5		Week 10	
Graft Type		**HY Mismatch**	**Gender Matched**	**HY Mismatch**	**Gender Matched**	**HY Mismatch**	**Gender Matched**
Correlation							
LFI *vs.* Number CD4$^+$ cells in graft	***p***	**0.0218** *	**0.0028** **	0.2972	N/A	0.2972	N/A
	R^2	**0.8016**	**0.9987**	0.05537		0.7907	
	r_s	**-0.8**	**1**	-0.5		0.5	
LFI *vs.* Number CD8$^+$ cells in graft	***p***	**<0.0001** ****	**0.0028** **	0.2972	N/A	**0.0218** *	N/A
	R^2	**0.9513**	**0.9199**	0.05537		**0.7758**	
	r_s	**1**	**1**	-0.5		**0.8**	
LFI *vs.* Number CD68$^+$ cells in graft	***p***	0.3268	**0.0469** *	**0.0028** **	N/A	**0.0028** **	N/A
	R^2	0.007507	**0.6682**	**0.7409**		**0.9864**	
	r_s	-0.4	**-1**	**1**		**1**	
Myocardial Vessel Area *vs.* *Number* CD4$^+$ cells in graft	***p***	**0.0287** *	**0.0004** ***	0.2012	0.3333	**0.0206** *	0.7639
	R^2	**0.5774**	**0.8901**	0.3686	1	**0.6903**	0.3286
	r_s	**-0.8**	**1**	0.5	-1	**0.6981**	-0.434
Subepicardial Vessel Area *vs.* Number CD4$^+$ cells in graft	***p***	**<0.0001** ****	**0.0016** ***	0.7316	0.3333	0.0594	0.4591
	R^2	**0.9354**	**0.8305**	0.03274	1	0.5414	0.1139
	r_s	**1**	**1**	-0.5	1	0.6981	0.06143
Myocardial Vessel Area *vs.* Number CD8$^+$ cells in graft	***p***	**<0.0001** ****	**0.0180** *	0.2012	0.3333	**0.0060** **	**0.0029** **
	R^2	**0.9445**	**0.6345**	0.3686	1	**0.7423**	**0.9129**
	r_s	**1**	**1**	0.5	-1	**0.8**	**-0.5**
Subepicardial Vessel Area *vs.* Number CD8$^+$ cells in graft	***p***	**0.0008** ***	0.0586	0.7316	0.4222	**0.0004** ***	0.1192
	R^2	**0.8368**	0.4752	0.0327	1	**0.8923**	0.4943
	r_s	**1**	1	**-0.5**	1	**0.8**	-0.5
Myocardial Vessel Area *vs.* Number CD68$^+$ cells in graft	***p***	**0.0016** **	0.1288	0.2250	**0.0222** *	0.1734	**0.0381** *
	R^2	**0.8329**	0.3406	0.3394	**0.8714**	0.2845	**0.8013**
	r_s	**-0.4**	-0.8	0.5	**-1**	-0.2	**-0.8**
Subepicardial Vessel Area *vs.* Number CD68$^+$ cells in graft	***p***	0.5620	0.0729	**0.0222** *	**0.0222** *	0.7064	**0.0048** **
	R^2	0.05906	0.4402	**0.9869**	**0.835**	0.02536	**0.9485**
	r_s	0.4	-0.8	**1**	**1**	-0.2	**-0.9487**
Myocardial Vessel number *vs.* Number CD68$^+$ cells in graft	***p***	0.1052	**0.0365** *	0.3486	0.3861	**<0.0001** ****	0.2677
	R^2	0.3773	**0.5449**	0.2195	0.1911	**0.9296**	0.1992
	r_s	0.4	**-0.8**	-0.5	0.5	**-0.8**	-0.6325

Europe PMC Funders Author Manuscripts

Time point		**Week 1**		**Week 5**		**Week 10**	
Graft Type		**HY Mismatch**	**Gender Matched**	**HY Mismatch**	**Gender Matched**	**HY Mismatch**	**Gender Matched**
Subepicardial LV number *vs.* Number $CD68^+$ cells in graft	***p***	0.2152	0.2156	0.1310	0.4222	**0.0169** *	**0.0493** *
	R^2	0.2424	0.2643	0.4731	0.9919	**0.6412**	**0.5015**
	r_s	0.6	0.6	-0.7379	0.5	**-1**	-1

R^2- using linear regression analyses; **r_s-** Spearman rank correlation coefficient;

p- probability calculated by spearman rank correlation

(* P ≤ 0.05 ** P ≤ 0.01 *** P ≤ 0.001 **** P ≤ 0.0001)